No-guard-band integration of digital coherent CV-QKD system into 400 Gbit/s 75 GHz grid DWDM systems

Tetsuo Kawakami,* Hiroki Kawahara, Toshihiko Okamura, Ken-ichiro Yoshino, and Wakako Maeda
Advanced Network Research Laboratories, NEC Corporation, Kawasaki, Kanagawa, Japan
(*) tetsuo-kawakami@nec.com

Abstract: We demonstrated no-guard-band integration of a digital coherent Continuous-variable QKD system into OpenZR$^+$-compliant DWDM transmission systems. The estimated secret key rate was 19.9 kbit/s over a 75 km EDFA amplified SMF link.

1. Introduction

Quantum key distribution (QKD) in combination with one-time pad encryption guarantees unconditional security by quantum mechanics. Continuous-variable (CV) QKD has attracted much attention among various QKD protocols because it can be implemented with off-the-shelf hardware from coherent communication technology. A traditional self-homodyne CV-QKD transmitter sends high-power local oscillator (LO) pulses to a receiver for optical carrier recovery, in which the attenuation of the traveled LO pulses limits the transmission distance [1]. Recent CV-QKD schemes have the LO at the receiver side to overcome this limit. Moreover, digital coherent CV-QKD, which enables carrier recovery based on digital signal processing (DSP), has been actively studied [2-3].

Regarding the practical deployment of QKD systems, integrating existing wavelength-division-multiplexing (WDM) transmission systems and the QKD system requiring a dedicated transmission line is highly desirable. Much research has demonstrated the coexistence of a self-homodyne CV-QKD signal with classical signals within the 1550-nm band to minimize the attenuation of a quantum signal [4-6]. However, the allocation of the self-homodyne CV-QKD channel into one specific frequency slot requires guard-band slots on both sides of the CV-QKD channel to avoid the nonlinear effect induced by the high-power LO pulses on the classical channels, which seriously decreases a spectral-efficiency of the existing WDM systems. The digital coherent CV-QKD has the potential to reduce the guard-band slots because it does not need to transmit the high-power LO pulse. For such a digital coherent CV-QKD channel, it is important to evaluate excess noise, which is the critical parameter of the secret key generation, even under the presence of the in-band noise induced by the coexistence with WDM signals.

In this paper, we demonstrate no-guard-band integration of a digital coherent CV-QKD system into OpenZR$^+$-compliant 400 Gbit/s 75 GHz grid dense-WDM (DWDM) transmission systems [7], assuming nearly realistic system conditions such as total launch power of +16 dBm and amplified single-span 75 km link. We also reveal that spontaneous-Raman-scattering (SpRS) lights induced from WDM signals dominate the QKD performance rather than amplified-spontaneous-emission (ASE) lights originating from a post-amplifier in the existing DWDM system and evaluate the excess noise of such SpRS-limited quantum signal to estimate secret-key-rates (SKRs) in our CV-QKD based on DSP [8].

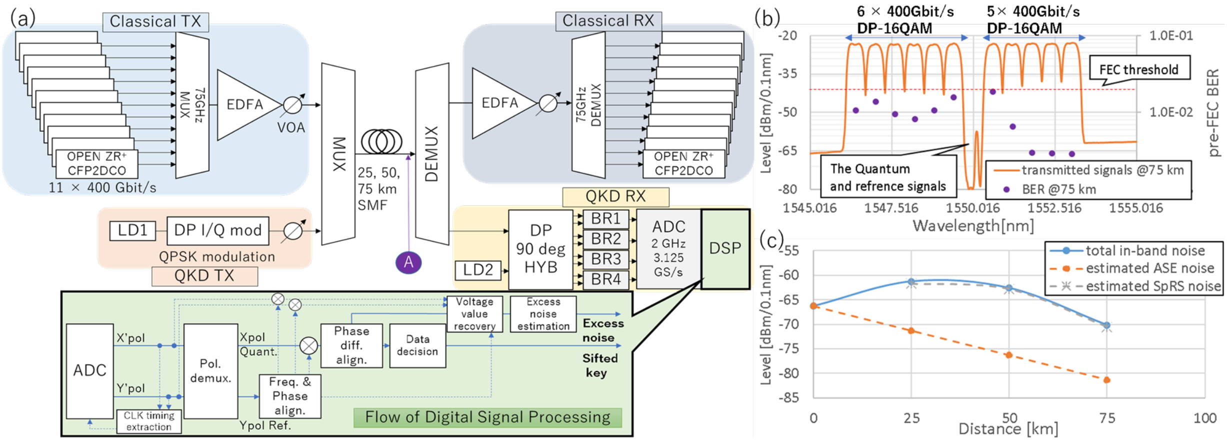

Fig. 1(a) Experimental setup. (b) Spectrum of the transmitted signals and pre-FEC BER of the 11 classical channels at 75 km at point A in Fig. 1a. (c) In-band noise power on the quantum signal.

2. Experimental setup

The experimental setup is shown in Fig. 1(a). In QKD TX, the transmitter Alice has a coherent light source tuned to 1550.12 nm. CV-QKD modulation using four phase states is implemented using a DP-I/Q-modulator, in which 1.25 GBaud RZ signals drive each polarization. The first (X-pol) and second polarization (Y-pol) are used for the quantum and a reference signal, respectively. We use the reference signal for carrier recovery of the quantum signal. We set the power of the reference signal to +30 dB higher than that of the quantum signal.

In QKD RX, the receiver Bob has a coherent light source used as true-local LO. A DP-90-degree hybrid is used, followed by four sets of balanced receivers with a bandwidth of 1.6 GHz. The transmitted signals are digitized using a 2 GHz bandwidth real-time oscilloscope with a 3.125 GS/s. The digitalized data is processed using a DSP algorithm for generating sifted keys. DSP includes clock timing extraction, polarization demultiplexing, frequency and phase alignment, and evaluation of the excess noise. We use half of the sifted keys to evaluate the excess noise and the other half to generate secret keys. Alice and Bob share the secret keys after applying Forward Error Correction (FEC) and Privacy Amplification to the sifted keys.

We co-propagate 75-GHz-spaced 11-channel 400 Gbit/s DP-16QAM signals and the quantum channel without guard-band slots over 0, 25, 50, and 75 km SMF links. The classical channels are sent and received by CFP2-DCO transceivers. They are amplified by erbium doped fiber amplifier (EDFA) and then launched into a transmission line with the total launch power of +16 dBm, corresponding to the channel power of +5.5 dBm. This excessive power condition equivalently simulates the SpRS noise generation in a fully (i.e., 63 channels) loaded system with channel power of -2 dBm. We use an add/drop filter for multiplexing (MUX) and demultiplexing (DEMUX) the quantum and classical signals. The center wavelength of the filter matches the WDM grids. The MUX exhibits a band-stop profile with a 3 dB bandwidth of 87 GHz and an isolation of 25 dB within the quantum signal band, sufficiently suppressing in-band ASE light. Similarly, the DEMUX has a band-pass profile with the same bandwidth and an isolation of 40 dB, effectively attenuating out-of-band classical signals.

3. Evaluation of excess noise of our DWDM system

It is necessary for generating secret keys to evaluate the excess noise by comparing the voltage variance of a shot noise and the quantum signal. In our CV-QKD based on DSP, after digital polarization demultiplexing, the voltage value of the signal is lost because of the amplitude normalization of the Constant Modulus Algorithm, and we cannot evaluate excess noise directly. We recover the voltage value of the quantum signal and evaluate excess noise by following steps. See the DSP flow of Fig. 1(a). First, the phase recovery of the pre-polarization demultiplexed signals is done by applying the phase tracking value of the reference signal. Then, the signal centers of the post-polarization demultiplexed signals are obtained by classifying the quadrature amplitude according to the reference signal data. Finally, we recover the voltage value of the quantum signal by comparing the signal centers before and after polarization demultiplexing.

4. Results and Discussion

The spectrum of the transmitted signals and the pre-FEC bit error rate (BER) of the classical channels are in Fig. 1(b). The measured FEC threshold of OFEC was 0.02, shown by the dotted line in Fig. 1(b). Although the pre-FEC BERs of the classical channels adjacent to the QKD channel were worse than that of other classical channels due to the signal spectral narrowing induced by slow roll-off of the add/drop filter, pre-FEC BERs in all channels did not exceed the FEC threshold. The measured in-band noise power on the quantum signal is in Fig. 1(c). The in-band noise power did not decrease monotonically with increasing distance because of the nonlinear SpRS lights, taking the worst value -61dBm/0.1 nm at 25 km. We estimated the ASE and the SpRS noise powers in Fig. 1(c) dotted line by assuming all in-band noise should be the ASE noise when the transmission distance is 0 km. Fig. 1(c)

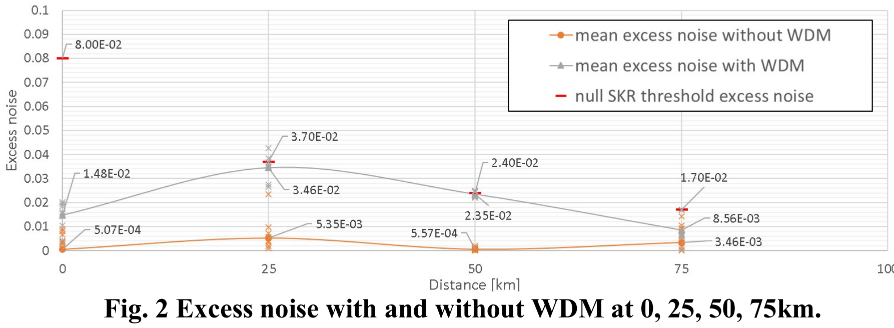

Fig. 2 Excess noise with and without WDM at 0, 25, 50, 75km.
The null threshold is calculated by the security analysis for the collective attacks [9].

shows that SpRS dominates the QKD performance in our DWDM system, no additional notch filtering for ASE noise suppression is required.

The evaluated excess noise with and without WDM is in Fig. 2. We measured each excess noise 8 times on block size 1×10^6. In Fig. 2, we plot each of 8 excess noises by the crosses, the mean excess noise by the solid line, and the null SKR excess noise by the bar. Owing to the in-band noise, the excess noise with WDM is worse than without WDM. While the excess noises without WDM were almost constant values even with increasing distance, the excess noises with WDM took the worst value at 25 km and became small with increasing distance, like the in-band noise power in Fig. 1 (c). All the mean excess noise was below the null SKR excess noise in Fig. 2.

The SKR is given as

$$SKR = f_p \eta_e \{\beta I(A|B) - \chi(E|B)\} \qquad \ldots(1)$$

where f_p is the Baud rate, η_e is the ratio of the training sequence, β is the reconciliation efficiency, $I(A|B)$ is the mutual information between Alice and Bob, and $\chi(E|B)$ is the Holevo information between Eavesdropper and Bob [9]. We set f_p = 1.25 GBaud, η_e = 0.5, and β = 0.95. The transmittance of the channel T at 0, 25, 50, and 75 km were 1, 0.316, 0.1, and 0.0316, respectively. The transmittance of the receiver η was 0.232. The electric noise of the detector v_{el} was 0.135. The mean number of photons on Alice's side n at 0, 25, 50, and 75 km were 0.35, 0.26, 0.22, and 0.24, respectively. The estimated SKRs with and without WDM are in Fig. 3. The SKRs are very sensitive to excess noise, so the SKRs were significantly worse at 25 and 50 km, in which in-band noise power was high and the excess noise was large. We succeeded in over 19.9 kbit/s secret key generation up to 75 km.

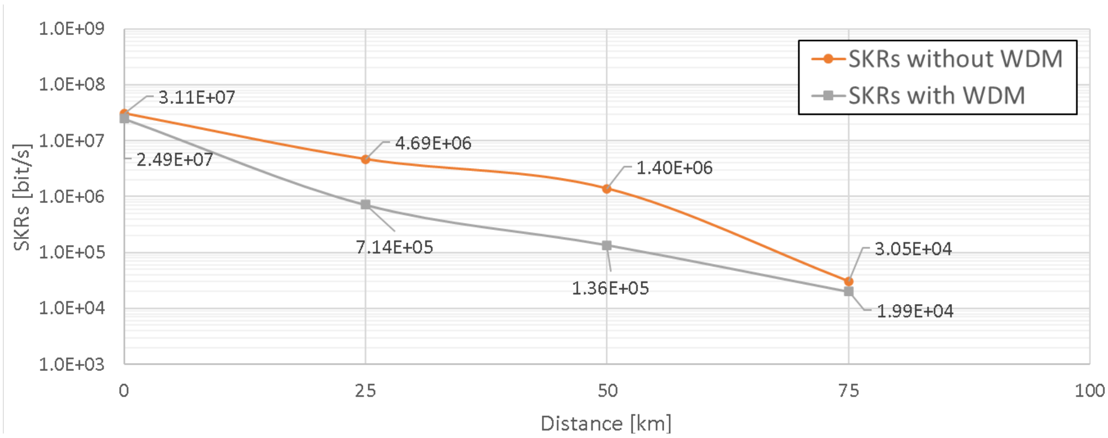

Fig. 3 Estimated SKRs with and without WDM

5. Conclusion

We demonstrated no-guard-band integration of the CV-QKD signal and 11-channel 75 GHz-spaced WDM signals with a total power of +16 dBm, which has a potential capacity of 25.2 Tbit/s (63 × 400 Gbit/s) as a fully loaded system with a channel power of -2 dBm. Our CV-QKD system successfully generated more than 19.9 kbit/s secret keys up to 75 km.

Acknowledgments

The work was partially supported by "Research and development for construction of a global quantum cryptography network" (JPJ008957) in "R&D of ICT Priority Technology Project" (JPMI00316) of the Ministry of Internal Affairs and Communications (MIC), Japan.

References

[1] T. Hirano et al., "Implementation of continuous-variable quantum key distribution with discrete modulation," Quantum Sci. Technol. 2 024010 (2017).
[2] T. A. Eriksson et al., "Digital self-coherent continuous variable quantum key distribution system," OFC.2020.T3D.5 (2020).
[3] H. Wang et al., "Sub-Gbps key rate four-state continuous-variable quantum key distribution within metropolitan area," Commun Phys 5, 162 (2022).
[4] R. Kumar et al., "Coexistence of continuous variable QKD with intense DWDM classical channels," New J. Phys. 17 043027 (2015).
[5] T. A. Eriksson et al., "Joint Propagation of Continuous Variable Quantum Key Distribution and 18 24.5 Gbaud PM-16QAM Channels," ECOC (2018).
[6] T. A. Eriksson et al., "Wavelength division multiplexing of continuous variable quantum key distribution and 18.3 Tbit/s data channels," Commun. Phys., 2, 9 (2019).
[7]D. Tauber et al., "Role of coherent systems in the next DCI generation," J. Lightw. Technol., 41, 4, (2023).
[8] T. Kawakami et al., "High Spectral Efficiency Digital Coherent Continuous Variable Quantum Key Distribution System Using Polarization-Multiplexed QPSK Reference Signal," ECOC (2023)
[9]H. Zhang et al., "Improving the performance of the four-state continuous-variable quantum key distribution by using optical amplifiers," Phys. Rev. A 86, 022338 (2012).